HHS Public Access

Author manuscript

Vet Microbiol. Author manuscript; available in PMC 2024 March 07.

Published in final edited form as:

Vet Microbiol. 2024 January ; 288: 109932. doi:10.1016/j.vetmic.2023.109932.

Carnitine palmitoyl-transferase 1A is potentially involved in bovine herpesvirus 1 productive infection

Hao Yang[a,1], **Wenyuan Gu**[b,1], **Junqing Ni**[c], **Yabin Ma**[c], **Shitao Li**[d], **Donna Neumann**[e], **Xiuyan Ding**[a,*], **Liqian Zhu**[a,*]

[a]College of Life Sciences, Hebei University, Baoding 071002, China

[b]Center for Animal Diseases Control and Prevention of Hebei Province, Shijiazhuang 050035, China

[c]Hebei Province Animal Husbandry and Improved Breeds Work Station, Shijiazhuang 050061, China

[d]Department of Microbiology and Immunology, Tulane University, New Orleans, LA 70118, USA

[e]Department of Ophthalmology and Visual Sciences, University of Wisconsin-Madison, Madison, WI 537006, USA

Abstract

Bovine herpesvirus 1(BoHV-1) is an important bovine pathogen that causes great economic loss to cattle farms worldwide. The virus-productive infection in bovine kidney (MDBK) cells results in ATP depletion. The mechanisms are not well understood. Mitochondrial fatty acid β-oxidation (FAO) is an important energy source in many tissues with high energy demand. Since carnitine palmitoyl-transferase 1 A (CPT1A) is the rate-limiting enzyme of FAO, we investigated the interactions between virus-productive infection and CPT1A signaling. Here, we found that virus-productive infection at the later stage significantly decreased CPT1A protein levels in all the detected cells, including MDBK, A549, and Neuro-2A cells, differentially altered the accumulation of CPT1A proteins in the nucleus and cytosol, and re-localized the protein in the nucleus. Etomoxir (ETO), an irreversible inhibitor of CPT1A, inhibited viral replication and partially interfered with the ability of BoHV-1 to alter CPT1A accumulation in the nucleus but not in the cytosol. Furthermore, ETO consistently reduced RNA levels of two viral regulatory proteins

*Corresponding author: lzhu3596@163.com (L. Zhu).

[1]These authors contributed equally to this work.

Author contributions

H.Y. generated the figures. W.Y.G., X.Y.D., and L.Q.Z. performed data analysis and manuscript preparation. L.Q.Z. and X.Y.D. designed and condensed this study. W.Y.G., X.Y.D., J.Q.N., and L.Q.Z. provided the funding. D.N., S.T.L., W.Y.G., and L.Q.Z. revised the manuscript.

Declaration of Competing Interest

The authors declare no conflicts of interest.

CRediT authorship contribution statement

Ma Yabin: Investigation, Resources. **Li Shitao:** Writing – review & editing. **Neumann Donna:** Methodology, Writing – review & editing. **Ding Xiuyan:** Project administration, Resources, Supervision, Writing – original draft. **Zhu Liqian:** Conceptualization, Data curation, Formal analysis, Funding acquisition, Project administration, Resources, Validation, Writing – original draft, Writing – review & editing. **Yang Hao:** Data curation, Investigation, Methodology. **Gu Wenyuan:** Funding acquisition, Investigation, Writing – original draft. **Ni Junqing:** Funding acquisition, Methodology, Resources.

(bICP0 and bICP22) and protein expression of virion-associated proteins during productive infection, further supporting the important roles of CPT1A signaling in BoHV-1 productive infection. These data, for the first time, suggest that CPT1A is potentially involved in BoHV-1 productive infection.

Keywords

BoHV-1; Etomoxir; CPT1A; β-oxidation

1. Introduction

Bovine herpesvirus 1 (BoHV-1), an enveloped DNA virus belonging to the family *Herpesviridae* and the subfamily *Alphaherpesvirinae*, is an important pathogen of cattle that causes severe diseases in cattle of all ages and breeds (Muylkens et al., 2007; Tikoo et al., 1995). The virus infection-induced suppression of the host immune responses may lead to secondary infections by diverse pathogens, such as bovine respiratory syncytial virus (BRSV), parainfluenza-3 virus (PI3V), bovine coronaviruses, *Mannheimia haemolytica*, *Pasteurella multocida*, *Histophilus somni,* and *Mycoplasma* spp, which may consequently result in the life-threatening pneumonia known as bovine respiratory disease complex (BRDC), the most important disease in cattle (Fulton et al., 2016; Jones, 1998). In addition, the virus infection is closely associated with viral abortion storms in cattle farms in North America. Thus, BoHV-1 infection is causing great economic loss to the cattle industry worldwide. An early report indicates that BoHV-1 infection costs the US cattle industry approximately 3 billion dollars annually (Jones and Chowdhury, 2007).

We have previously reported that BoHV-1 productive infection results in mitochondrial dysfunction and ATP depletion (Fu et al., 2019; Zhu et al., 2016), which may contribute to infection-induced tissue damage. However, the mechanisms concerning these findings are not well understood. It is well known that fatty acids are important energy sources, catabolized primarily by fatty acid β-oxidation (FAO) in mitochondria. Since FAO produces more than three-fold as much ATP per mole as glucose oxidation, it is the preferred energy source for highly metabolized cells in physiological conditions (Kastaniotis et al., 2017). However, the abnormal FAO process is related to a series of diseases, such as obesity and type 2 diabetes (He et al., 2018). Carnitine palmitoyl transferase 1 A (CPT1A) is the key rate-limiting enzyme for the process of FAO (Prip-Buus et al., 2001; Rasmussen and Wolfe, 1999). Overexpression of the CPT1A protein was found to be related to the pathogenicity of diverse diseases. For example, it promotes the progression of ovarian cancer, nasopharyngeal carcinoma (Shao et al., 2016; Tan et al., 2018), and nonalcoholic steatohepatitis (Yang et al., 2021). Accumulating studies have indicated that CPT1A is an attractive therapeutic target for intervention of various diseases (Dai et al., 2018; Schlaepfer and Joshi, 2020).

Although the roles of FAO that played in virus infection have been extensively studied in various viruses, including fish nodavirus (Huang et al., 2020), vaccinia virus (Greseth and Traktman, 2014), influenza A virus (van Liempd et al., 2021), and HIV-1 (Loucif et al., 2021; Prip-Buus et al., 2001; Rasmussen and Wolfe, 1999), the effects of CPT1A

signaling on virus replication are poorly understood. So far, only one virus, Marek's Disease Virus (MDV), has been exclusively investigated regarding its interaction with the CPT1A (Boodhoo et al., 2020).

Here, we showed that BoHV-1 productive infection leads to depletion of CPT1A protein expression and re-localization of CPT1A protein. CPT1A-specific inhibitor ETO significantly reduced the virus-productive infection. Taken together, for the first time, we found that CPT1A may play an important role in BoHV-1 productive infection, which may affect the CPT1A signaling pathway.

2. Materials and methods

2.1. Cells and viruses

MDBK and A549(purchased from Chinese Model Culture Preservation Center, Shanghai, China), as well as Neuro-2A cells (kindly gift from Professor Dongli Pan, Zhejiang University), were routinely passaged and maintained in DMEM supplemented with 10% fetal bovine serum (FBS). BoHV-1 stain NJ-16–1 isolated from bovine semen samples (Zhu et al., 2017) was propagated in MDBK cells. Aliquots of virus stocks were stored at − 70 °C until use.

2.2. Antibodies and reagents

The following antibodies were used in this study: CPT1A rabbit polyclonal antibody (pAb) (cat# A5307), β-Actin rabbit mAb (cat# AC026), and β-Tubulin Rabbit pAb(cat# AC015) were bought from Abclonal Technology (Woburn, MA, USA). COXIV rabbit pAb(cat#4844 S), HRP conjugated goat anti-mouse IgG (cat# **707**6), and HRP labeled goat anti-rabbit IgG (cat# 7074) were purchased from Cell Signaling Technology (Danvers, MA, USA). LaminA/C mouse mAb (cat# sc-376248) was provided by Santa Cruz Biotechnology (Dallas, TX, USA). BoHV-1 gD mAb (cat#1B8-F11), BoHV-1 gC mAb (cat#F2), and goat anti-BoHV-1 serum (cat# PAB-IBR) were provided by VMRD Inc. (Pullman, WA, USA). Donkey anti-goat IgG H&L (HRP) (ca#ab97110) was supplied by Abcam (Cambridge, UK). Alexa Fluor 488®-conjugated goat anti-rabbit IgG (H + L) (cat# A-11008) was provided by Invitrogen Life Technologies (Waltham, MA, USA). CPT1A-specific inhibitor Etomoxir (cat#HY-50202) was ordered from MedChemExpress (Monmouth Junction, NJ, USA).

2.3. Western blotting analysis

Cell lysates of either whole cell extracts or cellular fractions, including mitochondria, nucleus, and cytoplasm, were prepared using RIPA lysis buffer (1 × PBS, 1% NP-40, 0.5% sodium deoxycholate, 0.1% SDS) supplemented with protease inhibitor cocktail. They were boiled in Laemmli sample buffer for 5 min, subsequently subjected to separation on SDS-PAGE (8% or 10%), and then transferred to polyvinylidene fluoride (PVDF) membranes. Immuno-reactive bands were developed using Clarity Western ECL Substrate (Bio-Rad, cat# 1705061).

The band intensity was quantitatively analyzed for the designated studies with the free software Image J program (https://imagej.nih.gov/ij/download.html (accessed on 1

December 2020). Significance was assessed with a student *t*-test by using GraphPad Prism software (v5.0). *P* values of less than 0.05 (*p < 0.05) were considered significant for all the calculations.

2.4. Immunofluorescence assay

MDBK cells in 8-well chamber slides (Nunc Inc., IL, USA) were either mock infected or infected with BoHV-1 (MOI = 0.1). After infection for 24 h (h), cells were fixed with 4% paraformaldehyde in PBS for 10 min at room temperature, permeabilized with 0.25% Triton X-100 in PBS for 10 min at room temperature, and blocked with 1% BSA in PBST for 1 h followed by incubation with CPT1A antibody in 1% BSA in PBST overnight at 4 °C. After three washings, cells were incubated with secondary antibody labeled with distinct fluorescent dyes for 1 h in the dark at room temperature. After three washings, DAPI (4′,6-diamidino-2-phenylindole) staining was performed to visualize nuclei. Slides were covered with coverslips using an antifade mounting medium (Electron Microscopy Sciences, cat# 50–247–04). Images were captured using a confocal microscope (Leica).

2.5. DNA purification and quantification of viral DNA by qPCR

Total genomic DNA was extracted from infected cells using a commercial viral DNA purification kit (Tiangen, cat# DP-348) following the manufacturer's instructions. Freshly prepared DNA was used as a template for real-time qPCR to measure viral DNA levels with gC-specific primers, as described above.

Analysis of GAPDH was used as an internal control. Real-time PCR was carried out using the ABI 7500 fast real-time system (Applied Biosystems, CA). The levels of the viral genome represented by gC were normalized to that of the GAPDH gene. The relative levels of the vial genome were calculated using the method ($2^{-\Delta\Delta CT}$) compared to the control.

2.6. RNA isolation and quantification of mRNA by qRT-PCR

Total RNA was extracted from virus-infected cells treated with DMSO control or ETO at indicated concentrations using a TRIzol LS reagent (Ambion, cat# 10296010) following the manufacturer's instructions. Freshly prepared total RNA (1 μg) was used as a template for synthesizing first-strand cDNA with commercial random hexamer primers using Thermoscript™ RT-PCR system Kit (Invitrogen, cat# 11146–024) following the manufacturer's instructions. The cDNA products were then used as templates for real-time quantitative PCR to measure mRNA levels of indicated genes with gene-specific primers. Primers used to detect bICP0, bICP22, and GAPDH were described elsewhere (Zhu and Jones, 2017).

Analysis of glyceraldehyde-3-phosphate dehydrogenase (GAPDH) mRNA was used as an internal control. Real-time PCR was carried out using the ABI 7500 fast real-time system (Applied Biosystems, CA). The expression levels of the tested genes were normalized to that of the GAPDH gene. The relative mRNA level of each gene was calculated using the method ($2^{-\Delta\Delta CT}$) compared to the control.

2.7. Data analysis

The graphs were produced using the GraphpadPrism software. Statistical analyses were performed by the GraphpadPrism program. Data were expressed as the means ± S.E.M. and analyzed with a two-tailed Student's *t*-test at a $P < 0.05$ significance level.

3. Results

3.1. BoHV-1 infection has effects on CPT1A protein expression

Whether and how BoHV-1 productive infection affects CPT1A signaling has not been well characterized. To investigate whether CPT1A plays a role during BoHV-1 productive infection, we initially detected the steady-state levels of CPT1A protein following infection of bovine kidney (MDBK) cells, which is widely used for studying the virus replication mechanism. Our data indicated that CPT1A protein levels were gradually reduced following virus infection, particularly at later stages (Fig. 1A). Quantitative analysis showed that at 16, and 24 h post-infection (hpi), the protein levels were reduced to 71.24% and 57.53% relative to the control, respectively (Fig. 1B). These data suggested that virus infection has effects on CPT1A protein expression.

We then determined whether this effect showed a cell type-specific phenomenon. The steady-state protein levels of CPT1A were examined in two further cell lines, A549 and Neuro-2A, infected with BoHV-1, which also support the virus productive infection (Cardoso et al., 2016; Fiorito et al., 2020; Qiu et al., 2021; Rodrigues et al., 2010; Thunuguntla et al., 2017). These two cells were infected at much higher MOI of 1 and 10, respectively, because the virus replication efficiency is much lower in these cell cultures. As observed in MDBK cells, BoHV-1 productive infection may lead to depletion of CPT1A protein in both A549 and Neuro-2A cells (Figs. 1C and 1E). After 24 and 36 h infection, CPT1A protein levels decreased to approximately 62.84% and 52.98%, respectively, compared to the mock-infected control in A549 cells (Fig. 1D). CPT1A protein levels were reduced to approximately 46.53% in Neuro-2A cells after infection for 36 h (Fig. 1F). These data suggested that BoHV-1 productive infection leads to the depletion of CPT1A protein in a cell type-independent manner.

Furthermore, MDBK and Neuro-2A cells were infected with increasing MOI ranging from 0.1 to 10 to detect the variation of CPT1A protein levels at 16 and 36 hpi. As a result, CPT1A protein levels gradually decreased, to an extent correlated with increasing MOI (Fig. 1G and I). In MDBK cells, CPT1A protein levels were reduced to approximately 67.12%, 52.89%, and 32.38% following infection with MOI of 0.1, 1, and 10, respectively (Fig. 1H). In Neuro-2A cells, CPT1A protein levels were decreased to 76.88% and 49.05% following infection with MOI of 1 and 10, respectively (Fig. 1J). These data suggested that BoHV-1 productive infection leads to depletion of CPT1A protein in an MOI-specific manner, validating that the virus infection could specifically decrease CPT1A protein expression levels.

3.2. BoHV-1 infection re-localized CPT1A protein

Since the later-stage virus infection significantly reduced CPT1A protein expression, we wondered whether virus infection influenced CPT1A subcellular localization. For that purpose, confocal microscopy was performed 24 h after infection. In mock-infected MDBK cells, CPT1A was primarily detected in the nucleus, which was evenly distributed and overlapped well with DAPI staining (Fig. 2 upper panels). After virus infection, the nuclear CPT1A protein was relocalized, making it look like several adjoining clusters with irregular shapes. Unlike the mock-infected cells, nuclear CPT1A staining did not overlap well with that of DAPI, making DAPI stand out and readily observed (Fig. 2 bottom panels). In addition, higher levels of CPT1A proteins were readily detected in virus-infected cytosol relative to that of mock-infected controls (Fig. 2). Of note, all these images were captured under the same conditions. Thus, we suggested that the virus infection may increase the accumulation of cytosol CPT1A.

Another independent method was employed to evaluate further the effects of virus infection on CPT1A localization in MDBK cells, in which cellular fractions of both cytosol and nucleus were purified using a commercial nucleus isolation kit and subjected to Western blotting. In consistency with what we observed in the IFA assay (Fig. 2), CPT1A protein can be detected in the cytoplasmic fractions by Western blot (Fig. 3A). Relative to the mock-infected controls, CPT1A protein levels were decreased to approximately 47.79% in the nucleus and increased approximately 2-fold in the cytoplasm after viral infection (Fig. 3B), confirming that virus infection increased accumulation of CPT1A in cytoplasm, which incorporated with the data of IFA assay. LaminA/C, a marker for nuclear protein, was not detected in the cytoplasmic fraction, and β-tubulin, a marker for cytoplasmic protein, was not detected in the nuclear fractions, suggesting that neither fraction was contaminated by the counterpart (Fig. 3A), which validates the findings that virus infection leads to re-localization of CPT1A protein.

3.3. BoHV-1 infection has no effects on the accumulation of CPT1A protein in mitochondria

A subset of CPT1A molecules reside in mitochondria and play an important role in β-oxidation of long-chain fatty acids (Samudio et al., 2010; Xu et al., 2003). We wondered whether virus infection affects the accumulation of CPT1A proteins in mitochondria. For this purpose, cellular fractions of mitochondria were purified using a commercial kit and subjected to immunoblot to detect the CPT1A protein. As a result, the protein levels of CPT1A protein were not changed in virus-infected mitochondria relative to the mock-infected controls (Fig. 4).

3.4. CPT1A-specific inhibitor Etomoxir can reduce BoHV-1 virus replication

Etomoxir (ETO) is a chemical inhibitor of FAO that has irreversible effects on inhibiting CPT1A activity (Xu et al., 2003). To understand whether CPT1A signaling plays a role in BoHV-1 productive infection, the impact of ETO at a concentration ranging from 1 to 5 μM on virus productive infection was analyzed in MDBK cells after infection for 24 h. ETO at a concentration of 5 μM did not show cytotoxic effects on MDBK cell cultures in the designated conditions, as determined by the trypan-blue exclusion test described by

Fiorito et al. (Fiorito et al., 2008) (Fig. 5A). As a result, relative to the DMSO control, 1 μM ETO had no effects on virus yield, while 2.5 or 5 μM ETO consistently reduced the virus production approximately by 0.9- and 1.5-log, respectively (Fig. 5B). The effect of ETO on BoHV-1 infection was then examined in A549 and Neuro-2A cells. The virus titers were decreased to approximately 1.12- and 1.24-log by 2.5 or 5 μM ETO, respectively, in A549 cells (Fig. 5C). While, in Neuro-2A cells, the virus titers were deceased to around 1-log by 5 μM ETO (Fig. 5D). 5 μM ETO did not show cytotoxicity in either A549 or Neruo-2A cells after treatment for 24 and 36 h, respectively (Fig. 5A). So the decrease of virus titers was not because of cytocoticity. Taken together, the CAT1A inhibitor, ETO, significantly reduced BoHV-1 replication in three permissive cell lines, MDBK, A549, and Neuro-2A cells.

Then, the effects of ETO on BoHV-1 replication were extensively characterized in MDBK cells. In line with the virus titers, the viral genome copies were reduced to approximately 68.8% and 60.9% by ETO at a concentration of 2.5 and 5 μM, respectively (Fig. 6A). These data consistently suggest that ETO can inhibit virus-productive infection.

The same as HSV-1, BoHV-1 gene expression is divided into three distinct phases during the lytic infection: immediate early (IE), early (E), and late (L) (Harkness et al., 2014; Honess and Roizman, 1974). The viral regulatory proteins of IE genes play critical roles in regulating the expression of both E and L genes during productive infection (Mossman and Smiley, 1999). The effects of ETO on viral IE gene expression were detected by using qRT-PCR. The mRNA levels of the detected viral IE genes of both bICP0 and bICP22 were reduced by 5 μM ETO, which were decreased to approximately 47.7% and 55.0%, respectively (Fig. 6B). The inhibition of viral IE (bICP0 and bICP22) gene transcription corroborates the findings that ETO inhibits virus replication.

In addition, the effects of ETO on the expression of viral glycoprotein of both gC and gD were detected by Western blot. We found that ETO at all the detected concentrations decreased the protein expression of both gC and gD in a dose-dependent manner (Fig. 6C). After treatment by 1, 2.5, and 5 μM of ETO, gC protein levels were reduced to approximately 70.11%, 41.22% and 26.85%, respectively. The gD protein levels were reduced to approximately 72.01%, 57.12%, and 42.31%, respectively, compared to the mock-treated control (Fig. 6C and D). Then, we performed additional studies to detect ETO's effects on the expression of virion-associated proteins. For this purpose, MDBK cells were infected with BoHV-1 for 24 h and treated with either DMSO control or ETO at increasing concentrations. Then, the cell lysates were subjected to Western blotting using a commercial antibody developed against BoHV-1 virions. As shown in Fig. 6E, the antibody readily recognized at least six virion-associated proteins with distinct molecular weights denoted by a, b, c, d, e, f, and g. The expression levels of all the detected viral proteins were reduced by ETO treatment in a dose-dependent manner. Notably, bands denoted by e, f, and g were rarely recognized when the cell cultures were treated with 5 μM of ETO. These data indicate that ETO may affect the viral protein expression, which further confirms that ETO could inhibit the virus-productive infection.

Taken these data together, CPT1A-specific inhibitor ETO reduced virus productive infection in MDBK cells, differentially affected viral IE gene expression, and inhibited the protein

expression of virion-associated proteins. Thus, CPT1A signaling may play an important role in the virus-productive infection.

3.5. ETO treatment rescued the depletion of nuclear CPT1A protein induced by virus-productive infection

Since our results demonstrated that CPT1A-specific inhibitor ETO inhibits virus-productive infection and virus infection leads to CPT1A protein depletion, further studies were performed to detect whether ETO affects CPT1A protein expression in the context of virus-productive infection. When the virus-infected MDBK cells were treated with ETO at increasing concentrations ranging from 1.0 to 5.0 μM, CPT1A protein levels that decreased by the virus infection at later stages were significantly restored by 5.0 μM of ETO (Fig. 7A and B). Compared to the mock-treated virus-infected control, CPT1A protein levels increased by approximately 32.3% after treatment with 5.0 μM of ETO (Fig. 7B).

Since virus infection reduced the accumulation of CPT1A protein in the nucleus and increased the accumulation in the cytoplasm, we investigated whether ETO affects CP1A accumulation in distinct cellular fractions. As a result, ETO treatment rescued the depletion of nuclear CPT1A protein induced by virus infection (Fig. 7C). Relative to the mock-treated controls, CPT1A protein levels in the nucleus were increased by approximately 28.42% in the context of virus infection (Fig. 7C and E). Of note, ETO had no effects on the accumulation of CPT1A protein in cytosol fractions in the context of virus infection (Fig. 7D and E), though ETO reduced virus replication (Fig. 5B). We suggested that the altered accumulation of nuclear CPT1A protein by ETO treatment may correlate with the decreased virus replication and vice versa, which further confirmed that CPT1A signaling is involved in BoHV-1 productive infection.

4. Discussion

Accumulating studies have indicated that viruses may interrupt or use the host metabolism to facilitate efficient viral replication. Fatty acids may serve as precursors for ATP production via mitochondrial fatty acid β-oxidation (FAO), a well-defined metabolic pathway that serves as a primary bioenergetic source in many tissues (Ma et al., 2018). CPT1A is a key rate-limiting enzyme of FAO (Schlaepfer and Joshi, 2020). Whether CPT1A signaling is involved in BoHV-1 productive infection is not well understood. Previous reports indicate that BoHV-1 productive infection results in mitochondrial dysfunction and ATP depletion (Fu et al., 2019; Zhu et al., 2016). Therefore, we want to address whether CPT1A signaling is involved in the virus infection. Here, for the first time, we showed that BoHV-1 productive infection may have effects on CPT1A signaling at later stages during virus infection by demonstrating that the virus productive infection reduced CPT1A protein levels and re-localized CPT1A protein (Figs. 1–3). Importantly, it is well established that mitochondria-associated CPT1A protein is involved in the regulation of fatty acid metabolism via catalyzing the rate-limiting step in the transport of long-chain acyl-CoAs from the cytoplasm to the mitochondrial matrix (Prip-Buus et al., 2001; Rasmussen and Wolfe, 1999). Here, we found that virus infection rarely affects the accumulation of CPT1A protein in the fractions of mitochondria (Fig. 4). So, whether virus infection has effects on

FAO-mediated fatty acids metabolism via manipulation of the CPT1A signal pathway is an interesting question, deserving extensive studies in the future.

It has been well characterized that Etomoxir (ETO), a chemical inhibitor, could specifically inhibit mitochondrial transportation of long-chain fatty acids via irreversible blockage of CPT1A activity (Samudio et al., 2010; Xu et al., 2003). ETO treatment of virus-infected cells could significantly decrease the virus-productive infection (Fig. 5), indicating that either CPT1A signaling or CPT1A-associated fatty acid metabolism may play an important role in virus-productive infection. Particularly, the CPT1A protein expression decreased following BoHV-1 productive infection (Fig. 1), making the mechanism of how CPT1A signaling is potentially involved in regulating BoHV-1 productive infection complicated.

When referring to the literature, we noticed that ETO is generally applied at much higher concentrations to inhibit CPT1A activity than that we used here. For example, ETO at a concentration of 200 μM has been used to inhibit FAO in radiation-resistant glioblastoma (RR GBM) cells (Samudio et al., 2010). In this study, we found that ETO at a concentration of 5 μM could significantly reduce the virus titer and rescue CPT1A protein depletion attributed to the virus productive infection at later stages (Fig. 7). Though chemical inhibitors at lower concentrations may have less off-target effects, siRNA-mediated knockdown of CPT1A protein expression remains to be performed to confirm the specific roles of CPT1A signaling that played in BoHV-1 replication when the DNA sequence of CPT1A gene of *Bos taurus* origin is available in GenBank.

MDV is an avian alphaherpesvirus. Among all the viruses, MDV is the only one virus to have been investigated whether CPT1A signaling is involved in the virus replication. Unlike BoHV-1, CPT1A signaling is not required for MDV replication because the ETO inhibitor does not affect MDV productive infection in cell cultures (Boodhoo et al., 2020). Here, we found that BoHV-1 infection led to the depletion of CPT1A protein in the detected cell lines, including MDBK, A549, and Neuro-2A cells (Fig. 1). And the chemical inhibitor ETO inhibits virus productive infection without cell specificity (Fig. 5). Together with that report, we suggested that the roles of CPT1A signaling that played in virus infection are virus-specific.

A given host protein's biological activities may vary with distinct subcellular locations. Currently, it has been reported that a subset of CPT1A protein is located in the mitochondrial outer membrane (Faye et al., 2007; Gobin et al., 2003), inside the mitochondrion (Gaudet et al., 2011; Prip-Buus et al., 2001), as well as the cell membrane (Ghosh et al., 2010). CPT1A protein in the mitochondria regulates the fatty acid metabolic process (Prip-Buus et al., 2001; Rasmussen and Wolfe, 1999). However, the biological functions of CPT1A protein in cytoplasmic membrane remain to be elucidated. Here, for the first time, we found that the CPT1A protein is abundantly expressed in the nucleus via two independent studies (Figs. 2 and 3). Though we currently do not know the biological activities of nuclear CPT1A implicated in either mock-infected cells or virus-infected cells, our data suggest that it is involved in the virus-productive infection because the morphology of nuclear CPT1A protein is changed following virus infection (Fig. 2). The accumulation of nuclear CPT1A protein is significantly reduced (Fig. 3), which is reversed by ETO

treatment which may partially account for the decreased virus yield (Figs. 5 and 7). To clarify the mechanism of how the nuclear CPT1A protein was re-localized and whether this re-localization is implicated in virus infection are interesting issues deserving further studies in the future.

In summary, in this study, for the first time, we report an interplay between CPT1A signaling and BoHV-1 productive infection. For the first time, we found that a subset of the CPT1A protein resides in the nucleus, where the accumulation is significantly reduced following virus infection at later stages. CPT1A-specific inhibitor ETO significantly inhibits the virus-productive infection in cell cultures and reverses the depletion of nuclear CPT1A protein induced by virus infection. These data suggested that the CPT1A protein may play an important role in the virus-productive- infection in vitro. These findings will shed light on a new important notion for the interaction between BoHV-1 replication and CPT1A signaling, which may add more knowledge toward understanding the virus pathogenicity.

Acknowledgments

This research was supported by the National Natural Science Foundation of China (Grant Nos. 31972655, 31472172, and 31772743 to L. Q.Z.), Natural Science Foundation of Hebei Province (Grant Nos. C2022201046 to L.Q.Z., and H2022201081 to X.Y.D.), Key Research and Development Program of Hebei Province (Grant No. 21326358D to J.Q.N.), the Cow Innovation Group of Hebei Province (grant Nos. HBCT2023180201 to L.Q.Z., and HBCT2023180101 to J.Q.N.), and the Core Grant for Vision Research from the NIH to the University of Wisconsin-Madison (DMN) (P30 EY016665).

References

Boodhoo N, Kamble N, Sharif S, Behboudi S, 2020. Glutaminolysis and glycolysis are essential for optimal replication of Marek's disease virus. J. Virol 94.

Cardoso TC, Rosa AC, Ferreira HL, Okamura LH, Oliveira BR, Vieira FV, Silva-Frade C, Gameiro R, Flores EF, 2016. Bovine herpesviruses induce different cell death forms in neuronal and glial-derived tumor cell cultures. J. Neurovirol 22, 725–735. [PubMed: 27311457]

Dai J, Liang K, Zhao S, Jia W, Liu Y, Wu H, Lv J, Cao C, Chen T, Zhuang S, Hou X, Zhou S, Zhang X, Chen XW, Huang Y, Xiao RP, Wang YL, Luo T, Xiao J, Wang C, 2018. Chemoproteomics reveals baicalin activates hepatic CPT1 to ameliorate diet-induced obesity and hepatic steatosis. Proc. Natl. Acad. Sci. USA 115, E5896–E5905. [PubMed: 29891721]

Faye A, Esnous C, Price NT, Onfray MA, Girard J, Prip-Buus C, 2007. Rat liver carnitine palmitoyltransferase 1 forms an oligomeric complex within the outer mitochondrial membrane. J. Biol. Chem 282, 26908–26916. [PubMed: 17650509]

Fiorito F, Marfe G, De Blasio E, Granato GE, Tafani M, De Martino L, Montagnaro S, Florio S, Pagnini U, 2008. 2,3,7,8-tetrachlorodibenzo-p-dioxin regulates bovine herpesvirus type 1 induced apoptosis by modulating Bcl-2 family members. Apoptosis 13, 1243–1252. [PubMed: 18696228]

Fiorito F, Nocera FP, Cantiello A, Iovane V, Lambiase S, Piccolo M, Ferraro MG, Santamaria R, De Martino L, 2020. Bovine herpesvirus-1 infection in mouse neuroblastoma (Neuro-2A) cells. Vet. Microbiol 247, 108762. [PubMed: 32768214]

Fu X, Jiang X, Chen X, Zhu L, Zhang G, 2019. The differential expression of mitochondrial function-associated proteins and antioxidant enzymes during bovine Herpesvirus 1 infection: a potential mechanism for virus infection-induced oxidative mitochondrial dysfunction. Mediat. Inflamm 2019, 7072917.

Fulton RW, d'Offay JM, Landis C, Miles DG, Smith RA, Saliki JT, Ridpath JF, Confer AW, Neill JD, Eberle R, Clement TJ, Chase CC, Burge LJ, Payton ME, 2016. Detection and characterization of viruses as field and vaccine strains in feedlot cattle with bovine respiratory disease. Vaccine 34, 3478–3492. [PubMed: 27108192]

Gaudet P, Livstone MS, Lewis SE, Thomas PD, 2011. Phylogenetic-based propagation of functional annotations within the Gene Ontology consortium. Brief. Bioinform 12, 449–462. [PubMed: 21873635]

Ghosh D, Lippert D, Krokhin O, Cortens JP, Wilkins JA, 2010. Defining the membrane proteome of NK cells. J. Mass Spectrom 45, 1–25. [PubMed: 19946888]

Gobin S, Thuillier L, Jogl G, Faye A, Tong L, Chi M, Bonnefont JP, Girard J, Prip-Buus C, 2003. Functional and structural basis of carnitine palmitoyltransferase 1A deficiency. J. Biol. Chem 278, 50428–50434. [PubMed: 14517221]

Greseth MD, Traktman P, 2014. De novo fatty acid biosynthesis contributes significantly to establishment of a bioenergetically favorable environment for vaccinia virus infection. PLoS Pathog 10, e1004021. [PubMed: 24651651]

Harkness JM, Kader M, DeLuca NA, 2014. Transcription of the herpes simplex virus 1 genome during productive and quiescent infection of neuronal and nonneuronal cells. J. Virol 88, 6847–6861. [PubMed: 24719411]

He F, Jin JQ, Qin QQ, Zheng YQ, Li TT, Zhang Y, He JD, 2018. Resistin regulates fatty acid beta oxidation by suppressing expression of peroxisome proliferator activator receptor gamma-coactivator 1alpha (PGC-1alpha). Cell Physiol. Biochem 46, 2165–2172. [PubMed: 29730652]

Honess RW, Roizman B, 1974. Regulation of herpesvirus macromolecular synthesis. I. Cascade regulation of the synthesis of three groups of viral proteins. J. Virol 14, 8–19. [PubMed: 4365321]

Huang Y, Zhang Y, Zheng J, Wang L, Qin Q, Huang X, 2020. Metabolic profiles of fish nodavirus infection in vitro: RGNNV induced and exploited cellular fatty acid synthesis for virus infection. Cell Microbiol 22, e13216. [PubMed: 32388899]

Jones C, 1998. Alphaherpesvirus latency: its role in disease and survival of the virus in nature. Adv. Virus Res 51, 81–133. [PubMed: 9891586]

Jones C, Chowdhury S, 2007. A review of the biology of bovine herpesvirus type 1 (BHV-1), its role as a cofactor in the bovine respiratory disease complex and development of improved vaccines. Anim. Health Res. Rev 8, 187–205. [PubMed: 18218160]

Kastaniotis AJ, Autio KJ, Keratar JM, Monteuuis G, Makela AM, Nair RR, Pietikainen LP, Shvetsova A, Chen Z, Hiltunen JK, 2017. Mitochondrial fatty acid synthesis, fatty acids and mitochondrial physiology. Biochim. Biophys. Acta Mol. Cell Biol. Lipids 1862, 39–48. [PubMed: 27553474]

Loucif H, Dagenais-Lussier X, Beji C, Cassin L, Jrade H, Tellitchenko R, Routy JP, Olagnier D, van Grevenynghe J, 2021. Lipophagy confers a key metabolic advantage that ensures protective CD8A T-cell responses against HIV-1. Autophagy 17, 3408–3423. [PubMed: 33459125]

Ma Y, Temkin SM, Hawkridge AM, Guo C, Wang W, Wang XY, Fang X, 2018. Fatty acid oxidation: an emerging facet of metabolic transformation in cancer. Cancer Lett 435, 92–100. [PubMed: 30102953]

Mossman KL, Smiley JR, 1999. Truncation of the C-terminal acidic transcriptional activation domain of herpes simplex virus VP16 renders expression of the immediate-early genes almost entirely dependent on ICP0. J. Virol 73, 9726–9733. [PubMed: 10559282]

Muylkens B, Thiry J, Kirten P, Schynts F, Thiry E, 2007. Bovine herpesvirus 1 infection and infectious bovine rhinotracheitis. Vet. Res 38, 181–209. [PubMed: 17257569]

Prip-Buus C, Thuillier L, Abadi N, Prasad C, Dilling L, Klasing J, Demaugre F, Greenberg CR, Haworth JC, Droin V, Kadhom N, Gobin S, Kamoun P, Girard J, Bonnefont JP, 2001. Molecular and enzymatic characterization of a unique carnitine palmitoyltransferase 1A mutation in the Hutterite community. Mol. Genet. Metab 73, 46–54. [PubMed: 11350182]

Qiu W, Ding X, Li S, He Y, Zhu L, 2021. Oncolytic bovine Herpesvirus 1 inhibits human lung adenocarcinoma A549 cell proliferation and tumor growth by inducing DNA damage. Int. J. Mol. Sci 22. [PubMed: 35008458]

Rasmussen BB, Wolfe RR, 1999. Regulation of fatty acid oxidation in skeletal muscle. Annu. Rev. Nutr 19, 463–484. [PubMed: 10448533]

Rodrigues R, Cuddington B, Mossman K, 2010. Bovine herpesvirus type 1 as a novel oncolytic virus. Cancer Gene Ther 17, 344–355. [PubMed: 19893594]

Samudio I, Harmancey R, Fiegl M, Kantarjian H, Konopleva M, Korchin B, Kaluarachchi K, Bornmann W, Duvvuri S, Taegtmeyer H, Andreeff M, 2010. Pharmacologic inhibition of fatty acid

oxidation sensitizes human leukemia cells to apoptosis induction. J. Clin. Investig 120, 142–156. [PubMed: 20038799]

Schlaepfer IR, Joshi M, 2020. CPT1A-mediated fat oxidation, mechanisms, and therapeutic potential. Endocrinology 161. [PubMed: 33213120]

Shao H, Mohamed EM, Xu GG, Waters M, Jing K, Ma Y, Zhang Y, Spiegel S, Idowu MO, Fang X, 2016. Carnitine palmitoyltransferase 1A functions to repress FoxO transcription factors to allow cell cycle progression in ovarian cancer. Oncotarget 7, 3832–3846. [PubMed: 26716645]

Tan Z, Xiao L, Tang M, Bai F, Li J, Li L, Shi F, Li N, Li Y, Du Q, Lu J, Weng X, Yi W, Zhang H, Fan J, Zhou J, Gao Q, Onuchic JN, Bode AM, Luo X, Cao Y, 2018. Targeting CPT1A-mediated fatty acid oxidation sensitizes nasopharyngeal carcinoma to radiation therapy. Theranostics 8, 2329–2347. [PubMed: 29721083]

Thunuguntla P, El-Mayet FS, Jones C, 2017. Bovine herpesvirus 1 can efficiently infect the human (SH-SY5Y) but not the mouse neuroblastoma cell line (Neuro-2A). Virus Res 232, 1–5. [PubMed: 28104451]

Tikoo SK, Campos M, Babiuk LA, 1995. Bovine herpesvirus 1 (BHV-1): biology, pathogenesis, and control. Adv. Virus Res 45, 191–223. [PubMed: 7793325]

van Liempd S, Cabrera D, Pilzner C, Kollmus H, Schughart K, Falcon-Perez JM, 2021. Impaired beta-oxidation increases vulnerability to influenza A infection. J. Biol. Chem 297, 101298. [PubMed: 34637789]

Xu FY, Taylor WA, Hurd JA, Hatch GM, 2003. Etomoxir mediates differential metabolic channeling of fatty acid and glycerol precursors into cardiolipin in H9c2 cells. J. Lipid Res 44, 415–423. [PubMed: 12576524]

Yang H, Deng Q, Ni T, Liu Y, Lu L, Dai H, Wang H, Yang W, 2021. Targeted inhibition of LPL/FABP4/CPT1 fatty acid metabolic axis can effectively prevent the progression of nonalcoholic steatohepatitis to liver cancer. Int. J. Biol. Sci 17, 4207–4222. [PubMed: 34803493]

Zhu L, Jones C, 2017. The high mobility group AT-hook 1 protein stimulates bovine herpesvirus 1 productive infection. Virus Res 238, 236–242. [PubMed: 28684158]

Zhu L, Yu Y, Jiang X, Yuan W, Zhu G, 2017. First report of bovine herpesvirus 1 isolation from bull semen samples in China. Acta Virol 61, 483–486. [PubMed: 29186966]

Zhu L, Yuan C, Zhang D, Ma Y, Ding X, Zhu G, 2016. BHV-1 induced oxidative stress contributes to mitochondrial dysfunction in MDBK cells. Vet. Res 47, 47. [PubMed: 27000063]

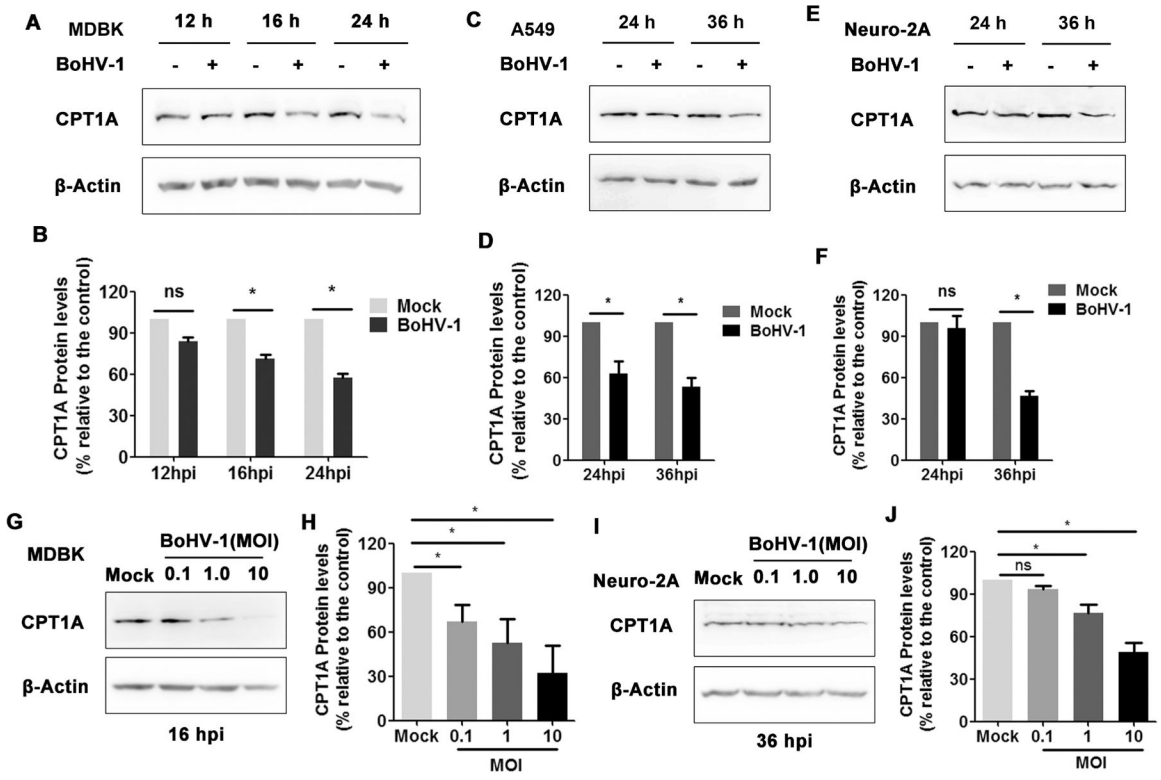

Fig. 1.

BoHV-1 infection in MDBK cells decreased the expression of CPT1A protein. MDBK (A), A549 (C), and Neuro-2A(E) cells were either mock infected or infected with BoHV-1 at an MOI of 0.1, 1, and 10, respectively, as routinely did, and at indicated time points, the cell lysates were prepared for western blotting to detect CPT1A. β-Actin was probed and used as a protein loading control and subsequent quantitative analysis. (G and I) MDBK(G) and Neuro-2A(I) cells were either mock infected or infected with BoHV-1 at an MOI of 0.1, 1, and 10, respectively. After infection for 16 h and 36 h, cell lysates of MDBK and Neuro-2A cells were prepared and subjected to Western blotting to detect the CPT1A protein, respectively. (B, D, F, H, and J) The band intensity was analyzed with free software image J. In detail, the band intensity of CPT1A was initially normalized to β-Actin, and the fold change after infection was calculated compared to that of mock-infected controls, which were arbitrarily set as 100%. The data shown are representative of three independent experiments with error bars indicating standard deviations. Significance was assessed with a student *t*-test (*$p < 0.05$, ns: not significant).

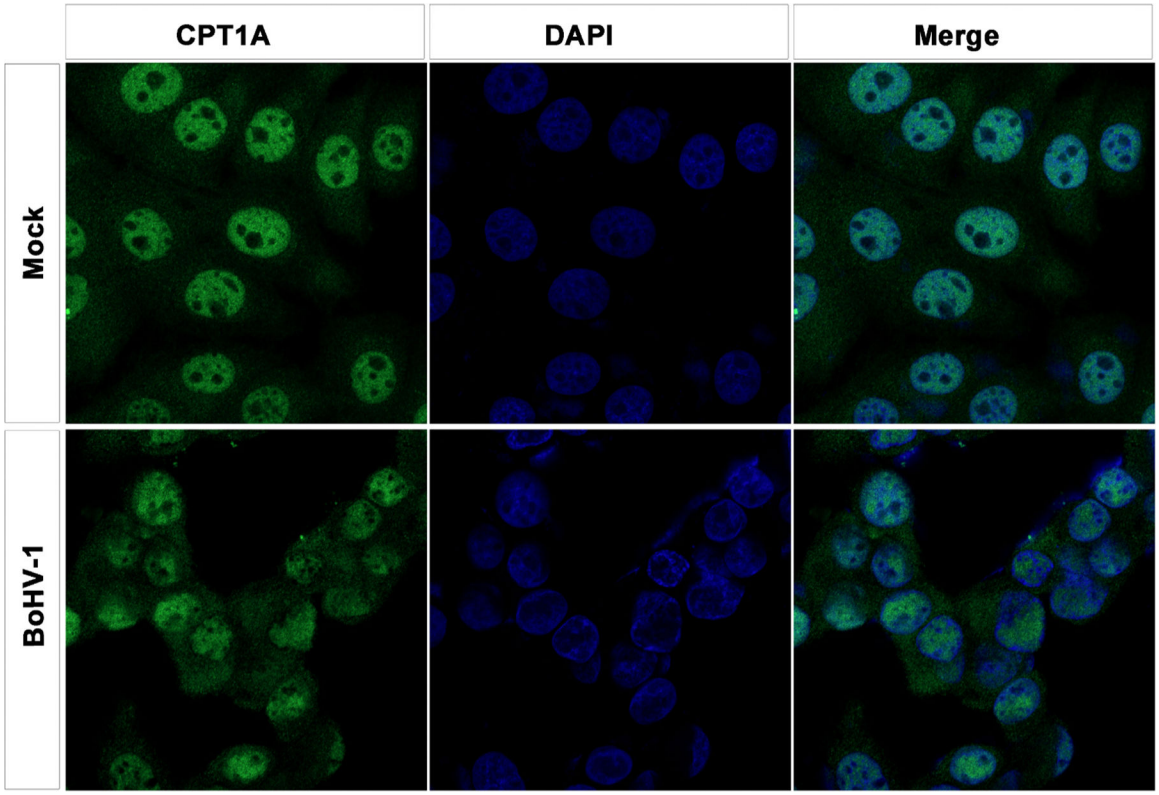

Fig. 2.

Subcellular localization of CPT1A protein in BoHV-1-infected MDBK cells. MDBK cells were either mock infected (upper panels) or infected (bottom panels) with BoHV-1 (MOI = 0.1) for 24 h. Then, they were stained with an antibody against CPT1A (green). Nuclei were stained with DAPI (4′,6-diamidino-2-phenylindole) (blue). Then, the immunostaining was visualized, and images were captured using confocal microscopy. These images are representative of those from three independent experiments.

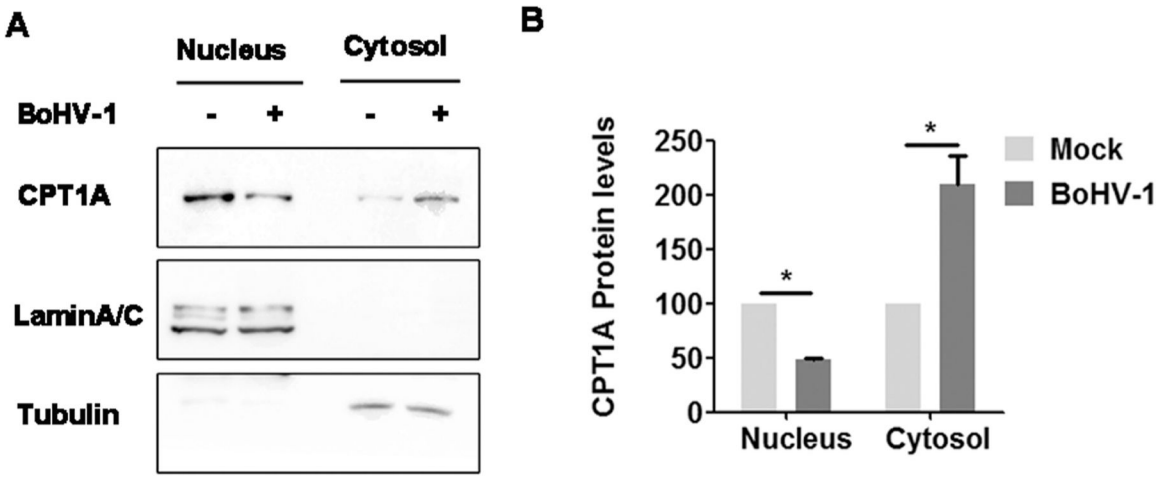

Fig. 3.

Effects that BoHV-1 infection had on nuclear accumulation of CPT1A proteins. (A) MDBK cells in 100 mm dishes were either mock-infected or infected with BoHV-1 (MOI = 0.1) for 24 h. The cells were collected to isolate both nucleus and cytosol fractions using a commercial kit (Beyotime Biotechnology, cat# P0027), following the manufacturer's protocol. Protein levels of CPT1A were detected by Western blotting. LaminA/C, a marker for nuclear protein, and β-tubulin, a marker for cytoplasmic protein, were detected as a protein loading control, respectively. (B) The band intensity was analyzed with free software image J. Band intensity of CPT1A was initially normalized to either LaminA/C or β-Actin, and the fold change after infection was calculated by comparison to that of mock-infected controls, which were arbitrarily set as 100%. The data shown are representative of three independent experiments with error bars indicating standard deviations. Significance was assessed with a student *t*-test (*$p < 0.05$).

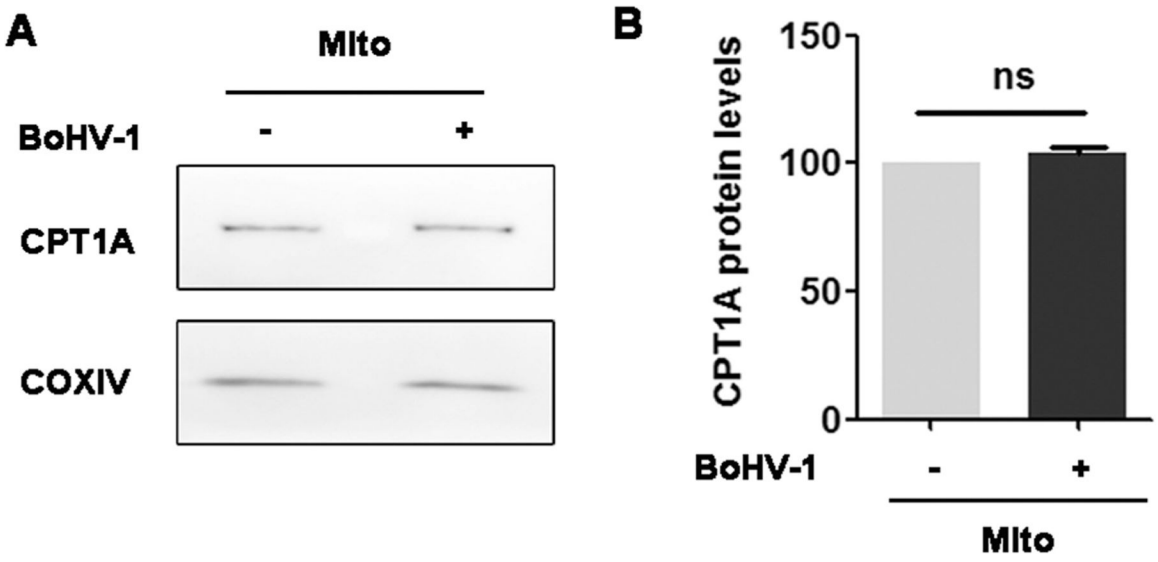

Fig. 4.

Effects of the BoHV-1 infection on the accumulation of CPT1A in mitochondria. (A) MDBK cells in 100 mm dishes were either mock-infected or infected with BoHV-1 (MOI = 0.1) for 24 h. The cells were collected to isolate mitochondria fractions via a commercial kit (Beyotime Biotechnology, cat# C3601) following the manufacturer's protocol. Protein levels of CPT1A were detected by Western blotting. COXIV was detected and used as a protein loading control. (B) Band intensity was analyzed with the software Image J. The control was arbitrarily set as 100%. The results shown are representations of three independent experiments. Error bars denote the variability between three independent experiments. Significance was assessed with a Student's t-test *t*-test (ns: not significant).

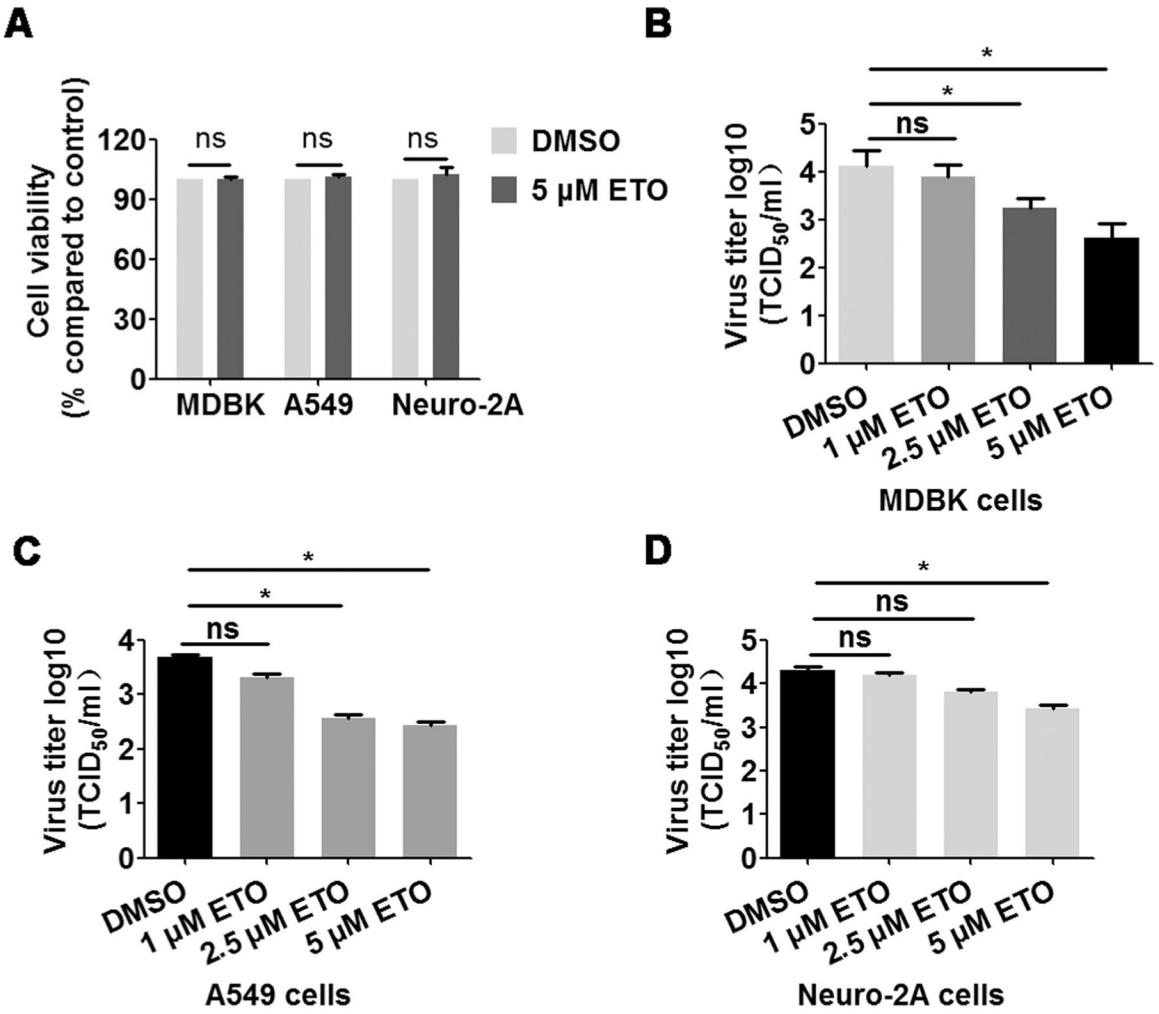

Fig. 5.

Effects of CPT1A-specific inhibitor ETO on BoHV-1 productive infection. (A) MDBK and A549 cells in 24-well plates were either mock-treated with DMSO control or with 5 μM of ETO for 24 h. Neuro-2A cells in 24-well plates were either mock treated with DMSO control or with 5 μM of ETO for 36 h. Then, cell viability was assessed by a Trypan-blue exclusion test. The cell number of mock-treated controls was arbitrarily set as 100%. MDBK(B), A549(C), and Neuro-2A(D) cells in 24-well plates were infected with BoHV-1 with MOI of 0.1, 1, and 10, respectively, along with treatment of either DMSO control or ETO at indicated concentrations. After infection for 24 h, the cell cultures of both MDBK and A549 cells were collected. After infection for 36 h, the cell cultures of Neuro-2A cells were collected. Then, virus titers were measured, and the results were expressed as $TCID_{50}$/mL.

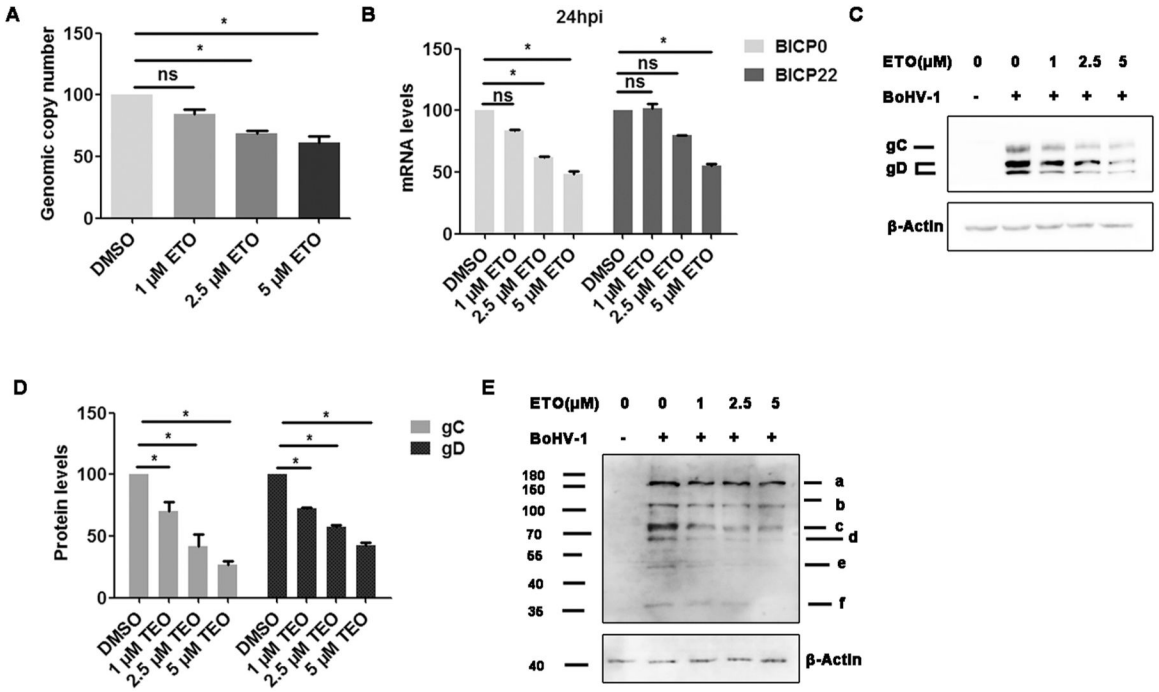

Fig. 6.

Effects of CPT1A-specific inhibitor ETO on viral gene expression (A) MDBK cells in 4-well plates were infected with BoHV-1(MOI = 0.1) and treated with DMSO vehicle or ETO at various concentrations. After infection for 24 h, genomic DNA was isolated and analyzed by relative qPCR to measure the viral genome through the detection of the gC gene. (B) As described in panel A, total RNA was isolated from virus-infected MDBK cells along with treatment of either DMSO control or ETO at indicated concentrations and analyzed by relative qRT-PCR to measure viral mRNA transcripts of bICP0 and bICP0. (C and D) MDBK cells in 6-well plates were either mock infected or infected with BoHV-1 along with treatment of either DMSO or ETO at indicated concentrations during virus infection. After infection for 24 h, cell lysates were prepared and subjected to Western blot to detect viral protein gC, gD, and virion-associated proteins. (E) Band intensity was analyzed with the software Image J. The control was arbitrarily set as 100%. Data represent the means of three independent experiments. Significance was assessed with Student's *t-test* (*$p < 0.05$, ns: not significant).

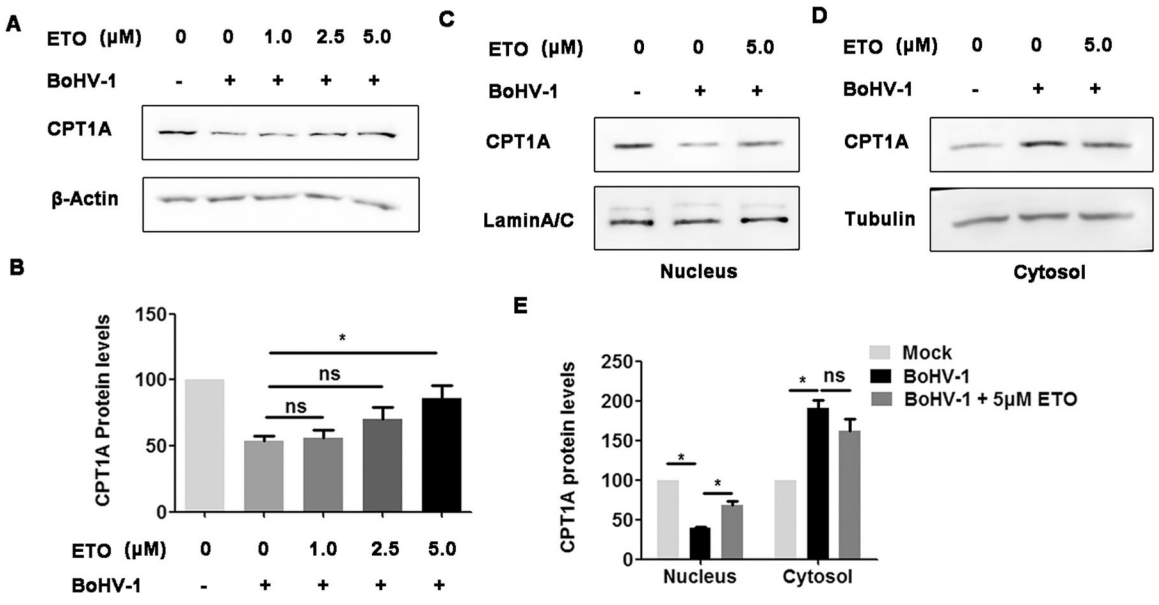

Fig. 7.

Effects of ETO on the expression and nucleus accumulation of CPT1A protein in virus-infected cells. (A) MDBK and in 60 mm dishes were mock infected or infected with BoHV-1 (MOI = 0.1) along with treatment of either vehicle control DMSO or ETO at indicated concentrations. After infection for 24 h, cell lysates were prepared and subjected to Western blot to detect CPT1A proteins. (C and D) MDBK cells in 100 mm dishes were either mock-infected or infected with BoHV-1 (MOI = 0.1), followed by mock treatment with DMSO control or 5 μM of ETO. After infection for 24 h, the cells were collected for isolation of both nucleus and cytosol fractions using a commercial kit (Beyotime Biotechnology, cat# P0027), following the manufacturer's protocol. Protein levels of CPT1A were detected from individual fractions by Western blotting. LaminA/C, a marker for nuclear protein, and β-tubulin, a marker for cytoplasmic protein, were detected as a protein loading control, respectively. (B and E) The band intensity was analyzed with free software image J. Data shown are representative results of three independent experiments with error bars indicating standard deviations. Significance was assessed with a student *t*-test (*$p < 0.05$, ns: not significant).